HHS Public Access

Author manuscript

J Cell Biochem. Author manuscript; available in PMC 2017 May 11.

Published in final edited form as:

J Cell Biochem. 2014 January ; 115(1): 121–129. doi:10.1002/jcb.24639.

Distinctive Subcellular Akt-1 Responses to Shear Stress in Endothelial Cells

Benoît Melchior and **John A. Frangos**

La Jolla Bioengineering Institute, San Diego, California 92121

Abstract

Endothelial cells undergo a rapid cell–cell junction inclination following exposure to atheroprotective unidirectional flow. In contrast, atherosclerotic lesions correlate with a heterogeneous distribution of the junctional wall inclination in cells exposed to time-varying, reversing, and oscillatory flow as well as to low mean shear stress. However, the underlying biochemical events by which endothelial cells distinctively respond to unidirectional versus flow reversal remain unclear. Here, we show that the subcellular distribution of flow-induced Akt-1 phosphorylation in endothelial cells lining the mouse aorta varies depending on local hemodynamics. Activated Akt-1 accumulated in perinuclear areas of cells in regions predisposed to disturbed flow but were localized at the cell–cell junction in regions of high unidirectional laminar shear stress. In flow-adapted human endothelial cells, reversal in flow direction was associated within minutes with a subcellular concentration of phosphorylated Akt-1 at the upstream edge of cells. Interestingly, oscillatory flow (with a zero mean shear stress) failed to activate Akt-1, whereas a unidirectional pulsatile flow of similar amplitude induced an increase in Akt-1 phosphorylation. Finally, silencing of the G protein $\alpha_{q/11}$ subunit abrogated both flow-induced Akt-1 and GSK-3β activation. Together, these results characterize the existence of a $G\alpha_{q/11}$-mediated Akt-1 signaling pathway that is dynamically responsive to flow direction, thereby offering a novel approach to regulating EC dysfunctions in regions subjected to flow reversal.

Keywords

Shear Stress; Endothelium; Akt-1; G Protein Alpha

Endothelial cells (EC) exposed to sustained laminar flow convey adaptive structural remodeling by elongating in the direction of flow [Dewey et al., 1981; Davies et al., 1995], a fusiform shape which correlates with low atherosclerotic susceptibility [DeBakey et al., 1985; Ku et al., 1985; Glagov et al., 1988; Garcia-Cardena et al., 2001; Hastings et al., 2007]. Although shape changes, cytoskeleton remodeling and subsequent cell alignment to a new flow direction may require hours, it was recently demonstrated that the endothelial cell–cell junction inclines in the direction of flow when subjected to unidirectional shear stress

Correspondence to: John A. Frangos.

Supporting Information: Additional supporting information may be found in the online version of this article at the publisher's web-site.

within 3 min [Melchior and Frangos, 2010]. Cells subjected to abrupt changes in flow direction rapidly reverse the cell–cell junction inclination and exhibit higher intracellular calcium responses [Melchior and Frangos, 2012].

Flow-reversal, or retrograde flow, has been described in normal physiological conditions in the inner curvature of the aortic arch [Suo et al., 2007]. Such events are particularly dramatic in cases of sudden vessel occlusions or surgically induced reverse flow such as in coronary artery bypass grafts where increased intimal hyperplasia has been implicated in decreased transplant tolerance [Haruguchi and Teraoka, 2003]. Similar retrograde flow is observed during carotid artery stent procedures designed to avert cerebral embolization [Pipinos et al., 2009]. The weakening in cardiac output observed in congestive heart failure also exposes part of previously flow-adapted endothelium to flow reversal during diastole [Gharib and Beizaie, 2003]. Longer exposure to flow reversal (or retrograde flow) modulates EC gene expression to a proinflammatory profile and induces production of reactive oxygen species [Passerini et al., 2003; Kassab et al., 2006]. However, the early cellular mechanisms by which cells subjected to shear can sense rapid changes in flow direction and convert the temporal gradients of local hemodynamics into intracellular signals remains to be elucidated.

The serine-threonine protein kinase Akt-1 (protein kinase B) is a critical intracellular mediator whose full activation through phosphorylation at Thr^{308} (T^{308}) and Ser^{473} (S^{473}) promotes growth factor-mediated cell survival and blocks apoptotic cell death [Alessi et al., 1996]. In EC, Akt-1 is responsive to laminar shear stress and promotes cell survival [Dimmeler et al., 1998], while Akt-1 deficient mice have profound increases in aortic lesions in an atherosclerogenic model [Fernandez-Hernando et al., 2007]. Here, we investigated the spatiotemporal activation of Akt-1 in EC subjected to various hemodynamic profiles and observed distinctive subcellular patterns of activation associated with flow direction. In vivo, a concentration of perinuclear phosphorylated Akt-1 was observed in EC at branch areas of the mouse aorta associated with disturbed local hemodynamics while the distribution of activated Akt-1 was primarily at the cell–cell junction in the descending aorta where flow is predicted to be unidirectional. In flow-adapted human umbilical vein EC (HUVEC), Akt-1 responses to step flow were localized at the upstream edge of the cells relative to the flow direction and were abrogated when the G protein $\alpha_{q/11}$ subunit ($G\alpha_{q/11}$) expression was reduced.

Materials and Methods

Cell Cultures and Treatments

HUVEC isolation was performed as previously described [Frangos et al., 1988]. Human umbilical cords were obtained from Sharp Memorial Hospital (San Diego, CA) under the auspices of Sharp Healthcare Institutional Review Board protocol no. 011081. Freshly harvested cells were cultured in flasks and then seeded onto glass microscope slides and grown to confluence within 4 days in M199 media (Irvine Scientific) supplemented with 20% fetal bovine serum. Prior to all experimental procedures, the HUVECs were serum-starved overnight in ATP-free M199 with 1% bovine serum albumin (BSA, Sigma-Aldrich, St. Louis, MO) to establish quiescence in the monolayer. Cells used as positive control for

Akt-1 activation were treated for 5 min with a combination 100 ng ml^{-1} final of VEGF (Biolegend, San Diego, CA) and 10 nM EGF (Peprotech, Rocky Hill, NJ).

Silencing of $G\alpha_{q/11}$ was performed using a siRNA target sequence common to both human $G\alpha_q$ and $G\alpha_{11}$ transcripts (sense: 5′-AAGATGTTCGTGGACCTGAA-3′). One hundred fifty nanomolars of final siRNA were combined to Lipofectamine siRNAmax (Invitrogen, Carlsbad, CA) according to the manufacturer's protocol and added to HUVEC for 5 h before cells were reseeded at high density onto slides for 2 days to allow cells to reestablish confluency.

Shear Stress Exposure

HUVEC monolayers were used in a conventional parallel-plate flow chamber where cells were subjected to a steady 16 dyn cm^{-2} fluid shear stress provided by a flow loop system maintained at 37°C and ventilated with 95% humidified air with 5% CO_2 [Frangos et al., 1988]. For flow adaptation, monolayers we subjected to 5 min slowly ramped up flow to 16 dyn cm^{-2}, followed by a 20 min steady flow period at 16 dyn cm^{-2} then a final 5 min ramping down period. This protocol was shown to quickly induce cell–cell junctional inclination in the direction of flow without activation of Akt-1, Erk1/2, intracellular calcium or $G\alpha_{q/11}$ [Melchior and Frangos, 2010, 2012]. Cells were then subjected to a 5 min step flow of similar magnitude in the same direction of flow adaptation (orthograde flow) or in the opposite direction (retrograde flow). Sham controls were not exposed to the last 5 min step flow but instead remained at 37°C. Static control slides were only removed from the incubator immediately prior to harvest or fixation.

Immunohisto- and Cytochemistry

Following flow stimulation, HUVEC were immediately fixed in ice-cold methanol for 5 min followed by 1 min in acetone then blocked in 5% normal goat serum and 1% BSA. Slides were then incubated overnight with a mouse monoclonal anti-human PECAM-1 antibody (R&D systems, Minneapolis, MN) and specific rabbit monoclonal antibodies against the phosphorylated Serine of Akt-1 at position 473 (S^{473}) or the phosphorylated threonine at position 308 (T^{308}) from Cell Signaling Technology (CST, Danvers, MA). This was followed by a final incubation with an anti-mouse Alexa Fluor 647 and a rabbit Alexa Fluor 488 antibody (Invitrogen) before slides were mounted in Vectashield (Vector Labs, CA). Monolayers were then examined under a confocal fluorescent microscope (Zeiss Pascal LSM5, Carl Zeiss, Jena, Germany) equipped with a Plan-Apochromatic 63/1.4 objective and a Plan-NEOFLUAR 100/1.3 objective and images were analyzed using the Zeiss LSM Image Browser.

For *en face* microscopy of phosphorylated Akt-1 in the aorta, four wild type C57Bl6/J mouse (Jackson Laboratory, Bar Harbor, ME) were anaesthetized with a cocktail of 90 mg kg^{-1} ketamine and 10 mg kg^{-1} xylazine, I.P., and rapidly perfused intracardially with 4% paraformaldehyde and 15% picric acid in cold PBS according to our institutional IACUC regulations. Aorta were then dissected under a stereoscopic binocular microscope from the aortic sinus to the renal artery bifurcation, cleaned of any fat residues and cut longitudinally in cold PBS before permeabilization with 0.3% Triton X-100. All initial steps including

incubation with the primary antibody were performed on ice and all solutions supplemented with 2 mM of the phosphatase inhibitor orthovanadate (Na_3VO_4). After blocking, vessels were incubated overnight with a rat monoclonal anti-mouse PECAM-1 from Biolegend and a Ser^{473} phospho-specific Akt-1 mouse monoclonal antibody from Rockland, Inc. (Gilbertsville, PA), then processed as described above.

Image Analysis

Phosphorylated Akt-1 perinuclear staining (green) and the length of PECAM-1 positive cells (red) was quantified in *en face* preparations using Image J software (NIH, USA). Each cell showing a full distinct ring of green staining around the nucleus was counted as a positive cell and a ratio was done over the total number of cells observed from at least three different fields of observation for each experiment. For localization of the phosphorylated Akt-1staining in vitro the upstream localization was defined as localization at the junction and immediately downstream of the junction according to flow direction. On the contrary, the phosphorylated Akt-1 staining was defined as downstream edge when found downstream of the cell and upstream of the cell–cell junction of the adjacent downstream cell.

Western Blot

Immediately following flow stimulation, slides were incubated for 1 min in ice-cold PBS plus Na_3VO_4 to prevent any dephosphorylation. Cells were then scraped off the slides, pelleted in ice-cold PBS then resuspended in 200 μl lysis buffer (60 mmol L^{-1} octyl glucoside, 50 mM Tris-HCl pH 7.5, 50 μmol L^{-1} EGTA, 125 mmol L^{-1} NaCl, 2 mmol L^{-1} dithiothreitol, 2 mmol L^{-1} Na_3VO_4 and protease inhibitors), and incubated on ice for 30 min. Lysates were centrifuged (14,000*g*, 20 min, 4°C) and the detergent-soluble supernatant fractions retained. Crude lysates were separated on NuPAGE 4-12% Bis-Tris gels (Invitrogen) and transferred to PVDF membrane (Millipore, Temecula, CA). Membranes were blocked for 1 h with 5% BSA in Tris-buffered saline with 0.1% (v/v) Tween 20 (TBST), and then incubated with a primary antibody for 1 h in 3% BSA-TBST. All antibodies were purchased from CST except total Akt-1 and β-tubulin antibodies were from Santa Cruz Technology (Santa Cruz, CA). Bound primary antibodies were detected by horseradish peroxidase-conjugated secondary antibodies anti-rabbit or anti-goat IgG True Blot (eBioscience, San Diego, CA). Band intensity was quantified on unsaturated X-ray film by a digital image analyzer (Bio-Rad Laboratories, Hercules, CA).

Statistics

Data are expressed as mean ± SEM from at least three independent experiments. Statistical comparisons between groups were performed using a one-tailed paired Student's *t*-test. A difference of $P < 0.05$ was judged significant and indicated on bar graphs with an asterisk.

Results

Accumulation of Perinuclear Pakt-1^{S473} in Regions of the Vasculature Prone to Disturbed Flow

Using en face immunohistochemistry in mouse aortas, a distinctive localization pattern of phosphorylated Akt-1 (pAkt-1^{S473}) was found. A diffused pAkt-1^{S473} staining was

observed throughout the small cells paving the brachiocephalic junction predicted to be exposed to low shear stress [Yoshida et al., 1995], whereas polygonal cells in regions of flow disturbances at bifurcation areas showed clear perinuclear pAkt-1 ^{S473} localization (Fig. 1A,B). Conversely, elongated EC in the descending aorta, a region of unidirectional shear stress, clearly revealed junctional localization of pAkt-1 ^{S473} and colocalized with PECAM-1 (Fig. 1C). An even more distinctive pattern was observed at the cell–cell junction in lateral branches where EC had an even further elongated geometry (Fig. 1D). A quantitative analysis of the pAkt-1 ^{S473} as a function of cell size showed that the pAkt-1 ^{S473} perinuclear accumulation was primarily found in polygonal cells defined with a diameter between 20 and 40 μm (78 ± 4%; Fig. 1F), while only 15 ± 1% of more elongated cells and 3 ± 0.4% of small cells with a diameter smaller than 20 μm showed any perinuclear staining (total number of cells counted: 129, 99, and 201, respectively).

Subcellular Location of Pakt-1 Related to Flow Direction

To investigate a potential relationship between pAkt-1 subcellular localization and hemodynamics, HUVEC monolayers were subjected to 5 min of a 16 dyn cm^{-2} step flow and immunostaining for pAkt-1 ^{S473} was performed. Remarkably, it was found that pAkt-1 ^{S473} was concentrated at the cell–cell junction and submembrane areas of the upstream edge of cells relative to the flow direction (Fig. 2A). By comparison, the pAkt-1 ^{S473} localization in resting cells (static condition) was absent, whereas that in cells subjected to a 5 min stimulation with a combination of 10 nM EGF and 100 ng ml^{-1} VEGF was observed to be uniformly expressed along the cell–cell junction (Fig. 2B).

It was previously shown that cells subjected to a change in flow direction rapidly adapt by inclination of their cell–cell junctions in the direction of flow [Melchior and Frangos, 2010]. We investigated whether subcellular localization of activated Akt-1 coincided with the inclination of the cell–cell junction. Cells were subjected to flow adaptation (a 30 min, non-stimulating slow ramping up and down) followed by a sudden 5 min ortho- or retrograde step flow (see protocol in Fig. 2C). A study of 49 fields of view from three independent experiments for a total of 476 cells analyzed indicated that the majority of cells (56 ± 2% cells on average per field) subjected to orthograde flow showed pAkt-1 ^{S473} localization almost uniquely present at the upstream edge of cells, mostly where cell–cell junctions laterally faced the direction of flow. Only 3% the cells showed downstream localization (Fig. 2D,F). The remaining 41% of cells did not show any or a residual diffused staining throughout the cell. When step flow was applied in the opposite direction to flow-adaptation, 30 ± 7% of the cells displayed pAkt-1 ^{S473} localization on the opposite edge, now the upstream submembrane areas relative to the new flow direction (Fig. 2E,F; total of 176 cells analyzed from 17 fields of view). It is worth noting that a large majority did not show any significant pAkt-1 ^{S473} activation with reversal of flow.

Akt-1 Phosphorylation was Attenuated with Flow Reversal

Akt-1 was phosphorylated at both Serine 473 (S^{473}) and Threonine 308 (T^{308}) upon a 5 min orthograde flow applied to flow-adapted endothelial monolayers (Fig. 3A,B, “Or”). Interestingly, flow-induced Akt-1 phosphorylation was reduced when cells were subjected to a change in flow direction (Retrograde (Re), reduction of 40% and 47% of Akt-1

phosphorylation at S^{473} and T^{308} sites, respectively). Moreover flow-induced activation of the Glycogen Synthase Kinase-3β (GSK-3β), a downstream effector of pAkt-1, in retrograde condition was completely abrogated (Fig. 3C). Shear-induced GSK-3β activation was mediated by Akt-1 activation as inhibition of Akt-1 phosphorylation inhibited the GSK-3β response to a 5 min step flow (Suppl. Fig. 1). In comparison, ERK was found to be insensitive to the flow direction as its phosphorylation was not found significantly different with orthograde or retrograde flow (Fig. 3D).

A Forward Flow Component Is Required for Akt-1 Activation

Although in vitro oscillatory flow does not reflect all the hemodynamic characteristics of in vivo disturbed flow, it shares the lack of junctional inclination [Melchior and Frangos, 2010]. When flow-naïve cells with a random distribution of the cell–cell junction inclination were subjected to repetitive changes in flow direction (oscillatory flow), no phosphorylation of Akt-1 at S^{473} was observed, whereas a dramatic increase was detected when the same sinusoidal flow profile of the same magnitude was applied but with an additional forward component (Pulsatile flow, no flow reversal, Fig. 4). In contrast, SRC was activated by both oscillatory and pulsatile flow profiles.

Flow-Induced Akt-1 Responses are Regulated by $G\alpha_{q/11}$

A previous investigation of the localization of $G\alpha_{q/11}$ in the aorta revealed a striking similarity to the pAkt-1 localization observed in Figure 1, with a distinct accumulation of $G\alpha_{q/11}$ in the perinuclear areas of EC exposed to disturbed flow and cell–cell junctional localization in areas subjected to unidirectional flow [Otte et al., 2009]. Here, we investigated whether these observations were correlated by silencing $G\alpha_q$ and $G\alpha_{11}$ transcripts in HUVEC. Interestingly, we found that silencing of the $G\alpha_{q/11}$ protein by siRNA in HUVEC dramatically abrogated pAkt-1 S^{473} responses (Fig. 5A,B). Similar responses were observed for the downstream Akt-1 effector GSK-3β (Fig. 5C).

Discussion

In this study, the subcellular distribution of activated serine-threonine protein kinase Akt-1 in endothelial cells subjected to various hemodynamics was investigated. We observed a distinctive pattern of Akt-1 in the mouse aorta in respect to regions with time-varying, disturbed, or low mean of shear stress. The activated/phosphorylated form of Akt-1 was predominantly found expressed at the cell–cell junction of elongated ECs lining the straight sections of the aorta and lateral vessels, areas known for unidirectional laminar shear stress. In contrast, ECs in regions predisposed to flow disturbances (near arterial branches, bifurcations and curvatures) expressed high levels of activated Akt-1 in perinuclear areas. Perinuclear pAkt-1 accumulation was recently described to be related to increased ubiquitination, a process affecting plasma recruitment of Akt-1 and nuclear trafficking [Fan et al., 2013]. In the present studies, the observed pattern of Akt-1 phosphorylation suggests a correlation between cell geometry, disturbed flow and a subcellular location of pAkt-1 defined by a perinuclear accumulation indicative of a proinflammatory phenotype or an early EC dysfunction. In contrast, elongated EC expressing distinctive cell–cell junction pAkt-1 localization correlated with an atheroprotective vascular localization. Interestingly,

samples from the brachiocephalic area (BCA, Fig. 1A) display smaller cell size along with a diffuse pattern of pAkt-1. The polygonal shape of these cells likely indicates the absence of unidirectional flow in this area. However, the difference in perinuclear pAkt-1 localization in the BCA compared to that found in larger polygonal cells of the renal artery bifurcation (Fig. 1B) may indicate that cells are subjected to different flow profiles such as oscillatory flow versus a reduced or a no flow profile.

The subcellular localization dependence on junctional inclination and flow direction suggests that membrane tension on the actin cytoskeleton plays a role in hemodynamic activation of Akt-1. In unidirectional flow, the region of greatest membrane tension is the endothelial cell–cell junction and the region immediately downstream of the junction [Fung and Liu, 1993; Melchior and Frangos, 2010]. This region also has increased actin filaments [Girard and Nerem, 1995], unless there is an increase in intracellular calcium as seen in retrograde flow [Melchior and Frangos, 2010] which destabilizes/depolymerizes the actin cytoskeleton [Prasain and Stevens, 2009]. Thus, in the case of retrograde flow, reduced upstream activation of Akt-1 is expected (Fig. 6).

In vivo pAkt-1 was localized over the entire cell perimeter in areas exposed to unidirectional shear (Fig. 1C,D), while only evident at cell junctions perpendicular to flow in vitro. This difference may be explained by a specific morphological flow adaptation of aligned cells that lack perpendicular walls exposed to flow but instead display a fusiform shape which allows membrane tension forces to be spread over a longer membrane surface than in polygonal cells whose perpendicular walls have yet to adapt. In addition, we have previously reported that the junctional inclination in regions of unidirectional flow is greater than that seen inflow-adapted endothelial cells in vitro [Melchior and Frangos, 2010]. The greater inclination implies reduced tension levels in vivo. Taken together, both shape and inclination differences in vivo and in vitro suggest reduced tension in vivo, which we speculate leads to reduced junctional pAkt-1 expression.

Physiologically, the reduced or absence of pAkt-1 survival signaling observed with sudden changes in shear stress correlate with increased atherosclerosis observed in Akt-$1^{-/-}$ mice [Fernandez-Hernando et al., 2007]. Specific loss of Akt-1 in endothelial cells results in reduced eNOS phosphorylation, NO release, endothelial cell migration and cell activation [Ackah et al., 2005; Chen et al., 2005; Phung et al., 2006]. Interestingly, Akt-1- and eNOS-deficient mice bred to an atherosclerotic background similarly lead to extensive coronary atherosclerosis with reduced eNOS phosphorylation, NO release, and endothelial cell migration [Kuhlencordt et al., 2001; Fernandez-Hernando et al., 2007]. The pAkt-1 subcellular distribution observed here also correlates with eNOS subcellular localization [Dusserre et al., 2004]. Hence, the loss of junctional Akt-1 activation observed at sites where atheromas develop is likely associated with disturbed hemodynamics, and lower cellular survival is likely due to the consequent decrease in NO bioavailability [Dimmeler et al., 1998]. Additionally, the distinctive pAkt-1 localization with flow reversal may be clinically relevant in regards to abrupt changes in flow direction induced during surgical procedures. These results highlight the need for a moderate flow adaptation of vessels during such surgical applications.

GSK-3β phosphorylation has previously been described in other mechanosensor pathways including the Wnt pathway in mechanically loaded bone cells [Robinson et al., 2006]. Here it was observed that flow-induced GSK-3β phosphorylation/deactivation in primary endothelial cells was mediated by Akt-1 phosphorylation. Similarly, application of force using magnetic microspheres coated with ligands to integrin subsets was found to be directly correlated with increased Akt-1 and GSK-3β phosphorylation when forces are applied laterally in the plane of the monolayer rather than downward [Chretien et al., 2010]. Mechanistically, a tight regulation of the inhibitory phosphorylation of GSK-3β is required for endothelial cell shear-induced shape change, and microtubule stabilization was previously shown to be shear-sensitive and GSK-3β-dependent [McCue et al., 2006]. Hence, it is possible that the decrease in GSK-3β phosphorylation observed during flow reversal could promote increased motility and cytoskeletal reorganization. These results are consistent with previous results showing an immediate remodeling of the cell–cell junctional interface following a sudden reversal of flow allowing the cell–cell junction to rapidly realign in the new flow direction [Melchior and Frangos, 2010].

Although decreased Akt-1 activation may be explained by activation of phosphatases during retrograde flow it was found here that flow-induced Akt-GSK3β responses were tightly regulated by the G protein $\alpha_{q/11}$ subunit. Reduction in $G\alpha_{q/11}$ levels almost completely abrogated flow-induced Akt-1 responses. Interestingly, it was previously observed that, similar to the pAkt-1 localization in vivo, $G\alpha_{q/11}$ is expressed in the perinuclear areas near arterial branches subjected to high flow disturbances while it is primarily localized at the cell–cell junction in the atheroprotected descending aorta [Otte et al., 2009]. Whether the differences observed between ortho- and retrograde flow-induced Akt-1 activation could be attributed to a decrease in $G\alpha_{q/11}$ activity during reversal flow remains unknown. However, $G\alpha_{q/11}$ is intimately associated to PECAM-1 at the cell–cell junction in a shear-dependent manner [Otte et al., 2009]. Indeed, temporal gradients of shear stress lead to a rapid dissociation and re-association of the $G\alpha_{q/11}$/PECAM-1 complex within 30 sec while transitioning fluid flow (slowly ramped flow) does not disrupt the complex. Moreover, PECAM-1 was found to regulate GSK-3β phosphorylation during shear stress [Biswas et al., 2006]. These data and those presented here imply the existence of a $G\alpha_{q/11}$ and PECAM-1 regulation of shear-induced Akt-GSK3β activation.

Together, our results indicate that (1) junctional localization of pAkt-1 correlates with regions of high unidirectional shear stress whereas a perinuclear localization correlates with areas of disturbed flow, and (2) Akt-1 activation is dynamically responsive to flow direction through a $G\alpha_{q/11}$-mediated pathway. Thus, the regulation of Akt-1 activation may provide a therapeutic approach to decrease EC dysfunction in regions subjected to flow reversal.

Supplementary Material

Refer to Web version on PubMed Central for supplementary material.

Acknowledgments

The authors would like to thank Drs. J.-C. Yeh and Nathaniel dela Paz for sustained technical help.

References

Ackah E, Yu J, Zoellner S, Iwakiri Y, Skurk C, Shibata R, Ouchi N, Easton RM, Galasso G, Birnbaum MJ, Walsh K, Sessa WC. Akt1/protein kinase B alpha is critical for ischemic and VEGF-mediated angiogenesis. J Clin Invest. 2005; 115:2119–2127. [PubMed: 16075056]

Alessi DR, Andjelkovic M, Caudwell B, Cron P, Morrice N, Cohen P, Hemmings BA. Mechanism of activation of protein kinase B by insulin and IGF-1. EMBO J. 1996; 15:6541–6551. [PubMed: 8978681]

Biswas P, Canosa S, Schoenfeld D, Schoenfeld J, Li P, Cheas LC, Zhang J, Cordova A, Sumpio B, Madri JA. PECAM-1 affects GSK-3beta-mediated beta-catenin phosphorylation and degradation. Am J Pathol. 2006; 169:314–324. [PubMed: 16816383]

Chen J, Somanath PR, Razorenova O, Chen WS, Hay N, Bornstein P, Byzova TV. Akt1 regulates pathological angiogenesis, vascular maturation and permeability in vivo. Nat Med. 2005; 11:1188–1196. [PubMed: 16227992]

Chretien ML, Zhang M, Jackson MR, Kapus A, Langille BL. Mechanotransduction by endothelial cells is locally generated, direction-dependent, and ligand-specific. J Cell Physiol. 2010; 224:352–361. [PubMed: 20432432]

Davies PF, Mundel T, Barbee KA. A mechanism for heterogeneous endothelial responses to flow in vivo and in vitro. J Biomech. 1995; 28:1553–1560. [PubMed: 8666594]

DeBakey ME, Lawrie GM, Glaeser DH. Patterns of atherosclerosis and their surgical significance. Ann Surg. 1985; 201:115–131. [PubMed: 3155934]

Dewey CF Jr, Bussolari SR, Gimbrone MA Jr, Davies PF. The dynamic response of vascular endothelial cells to fluid shear stress. J Biomech Eng. 1981; 103:177–185. [PubMed: 7278196]

Dimmeler S, Assmus B, Hermann C, Haendeler J, Zeiher AM. Fluid shear stress stimulates phosphorylation of Akt in human endothelial cells: Involvement in suppression of apoptosis. Circ Res. 1998; 83:334–341. [PubMed: 9710127]

Dusserre N, L'Heureux N, Bell KS, Stevens HY, Yeh J, Otte LA, Loufrani L, Frangos JA. PECAM-1 interacts with nitric oxide synthase in human endothelial cells: Implication for flow-induced nitric oxide synthase activation. Arterioscler Thromb Vasc Biol. 2004; 24:1796–1802. [PubMed: 15284089]

Fan CD, Lum MA, Xu C, Black JD, Wang X. Ubiquitin-dependent regulation of phospho-AKT dynamics by the ubiquitin E3 ligase, NEDD4-1, in the insulin-like growth factor-1 response. J Biol Chem. 2013; 288:1674–1684. [PubMed: 23195959]

Fernandez-Hernando C, Ackah E, Yu J, Suarez Y, Murata T, Iwakiri Y, Prendergast J, Miao RQ, Birnbaum MJ, Sessa WC. Loss of Akt1 leads to severe atherosclerosis and occlusive coronary artery disease. Cell Metab. 2007; 6:446–457. [PubMed: 18054314]

Frangos JA, McIntire LV, Eskin SG. Shear stress induced stimulation of mammalian cell metabolism. Biotechnol Bioeng. 1988; 32:1053–1060. [PubMed: 18587822]

Fung YC, Liu SQ. Elementary mechanics of the endothelium of blood vessels. J Biomech Eng. 1993; 115:1–12. [PubMed: 8445886]

Garcia-Cardena G, Comander JI, Blackman BR, Anderson KR, Gimbrone MA. Mechanosensitive endothelial gene expression profiles: Scripts for the role of hemodynamics in atherogenesis? Ann N Y Acad Sci. 2001; 947:1–6. [PubMed: 11795257]

Gharib M, Beizaie M. Correlation between negative near-wall shear stress in human aorta and various stages of congestive heart failure. Ann Biomed Eng. 2003; 31:678–685. [PubMed: 12797617]

Girard PR, Nerem RM. Shear stress modulates endothelial cells morphology and F-actin organization through the regulation of focal adhesion-associated proteins. J Cell Physiol. 1995; 163:179–193. [PubMed: 7534769]

Glagov S, Zarins C, Giddens DP, Ku DN. Hemodynamics and atherosclerosis. Insights and perspectives gained from studies of human arteries. Arch Pathol Lab Med. 1988; 112:1018–1031. [PubMed: 3052352]

Haruguchi H, Teraoka S. Intimal hyperplasia and hemodynamic factors in arterial bypass and arteriovenous grafts: A review. J Artif Organs. 2003; 6:227–235. [PubMed: 14691664]

Hastings NE, Simmers MB, McDonald OG, Wamhoff BR, Blackman BR. Atherosclerosis-prone hemodynamics differentially regulates endothelial and smooth muscle cell phenotypes and promotes pro-inflammatory priming. Am J Physiol Cell Physiol. 2007; 293:C1824–C1833. [PubMed: 17913848]

Kassab GS, Navia JA, Lu X. Proper orientation of the graft artery is important to ensure physiological flow direction. Ann Biomed Eng. 2006; 34:953–957. [PubMed: 16783651]

Ku DN, Giddens DP, Zarins CK, Glagov S. Pulsatile flow and atherosclerosis in the human carotid bifurcation. Positive correlation between plaque location and low oscillating shear stress. Arteriosclerosis. 1985; 5:293–302. [PubMed: 3994585]

Kuhlencordt PJ, Gyurko R, Han F, Scherrer-Crosbie M, Aretz TH, Hajjar R, Picard MH, Huang PL. Accelerated atherosclerosis, aortic aneurysm formation, and ischemic heart disease in apolipoprotein E/endothelial nitric oxide synthase double-knockout mice. Circulation. 2001; 104:448–454. [PubMed: 11468208]

McCue S, Dajnowiec D, Xu F, Zhang M, Jackson MR, Langille BL. Shear stress regulates forward and reverse planar cell polarity of vascular endothelium in vivo and in vitro. Circ Res. 2006; 98:939–946. [PubMed: 16527990]

Melchior B, Frangos JA. Shear-induced endothelial cell–cell junction inclination. Am J Physiol Cell Physiol. 2010; 299:C621–C629. [PubMed: 20554908]

Melchior B, Frangos JA. Galphaq/11-mediated intracellular calcium-responses to retrograde flow in endothelial cells. Am J Physiol Cell Physiol. 2012; 303:C467–C473. [PubMed: 22700794]

Otte LA, Bell KS, Loufrani L, Yeh JC, Melchior B, Dao DN, Stevens HY, White CR, Frangos JA. Rapid changes in shear stress induce dissociation of a G alpha(q/11)-platelet endothelial cell adhesion molecule-1 complex. J Physiol. 2009; 587:2365–2373. [PubMed: 19332487]

Passerini AG, Milsted A, Rittgers SE. Shear stress magnitude and directionality modulate growth factor gene expression in preconditioned vascular endothelial cells. J Vasc Surg. 2003; 37:182–190. [PubMed: 12514598]

Phung TL, Ziv K, Dabydeen D, Eyiah-Mensah G, Riveros M, Perruzzi C, Sun J, Monahan-Earley RA, Shiojima I, Nagy JA, Lin MI, Walsh K, Dvorak AM, Briscoe DM, Neeman M, Sessa WC, Dvorak HF, Benjamin LE. Pathological angiogenesis is induced by sustained Akt signaling and inhibited by rapamycin. Cancer Cell. 2006; 10:159–170. [PubMed: 16904613]

Pipinos II, Pisimisis GT, Burjonrappa SC, Johanning JM, Longo GM, Lynch TG. One patent intracranial collateral predicts tolerance of flow reversal during carotid angioplasty and stenting. Ann Vasc Surg. 2009; 23:32–38. [PubMed: 18619779]

Prasain N, Stevens T. The actin cytoskeleton in endothelial cell phenotypes. Microvasc Res. 2009; 77:53–63. [PubMed: 19028505]

Robinson JA, Chatterjee-Kishore M, Yaworsky PJ, Cullen DM, Zhao W, Li C, Kharode Y, Sauter L, Babij P, Brown EL, Hill AA, Akhter MP, Johnson ML, Recker RR, Komm BS, Bex FJ. Wnt/beta-catenin signaling is a normal physiological response to mechanical loading in bone. J Biol Chem. 2006; 281:31720–31728. [PubMed: 16908522]

Suo J, Ferrara DE, Sorescu D, Guldberg RE, Taylor WR, Giddens DP. Hemodynamic shear stresses in mouse aortas: Implications for atherogenesis. Arterioscler Thromb Vasc Biol. 2007; 27:346–351. [PubMed: 17122449]

Yoshida Y, Okano M, Wang S, Kobayashi M, Kawasumi M, Hagiwara H, Mitsumata M. Hemodynamic-force-induced difference of interendothelial junctional complexes. Ann N Y Acad Sci. 1995; 748:104–120. discussion 120–121. [PubMed: 7695160]

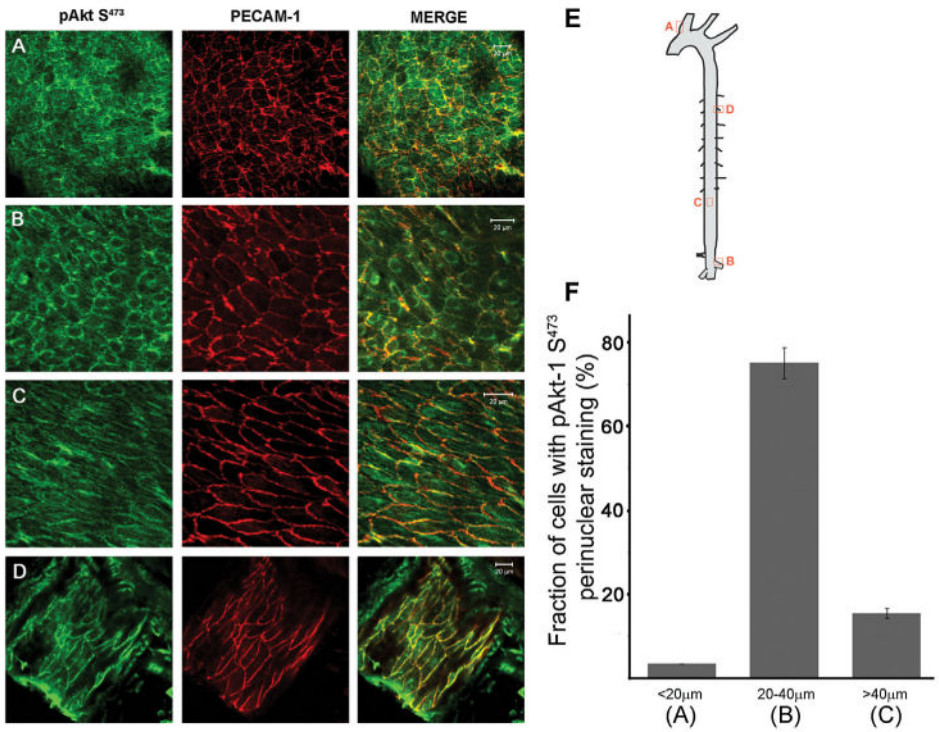

Fig. 1.

Cell morphology and spatiolocalization of phosphorylated Akt-1 in the mouse aorta. *En face* immunostaining of pAkt-1^{S473} (green) and PECAM-1 (red) in the brachiocephalic area (A), the renal artery bifurcation (B), the distal part of the descending aorta (C), and the adjacent intercostals artery (D). Scale bar is 20 μm. E: Sites along the aorta where samples were derived. F: Bar graph illustrating the fraction of EC expressing perinuclear pAkt-1^{S473} staining in regards to cell diameter from areas shown in a, b, and c.

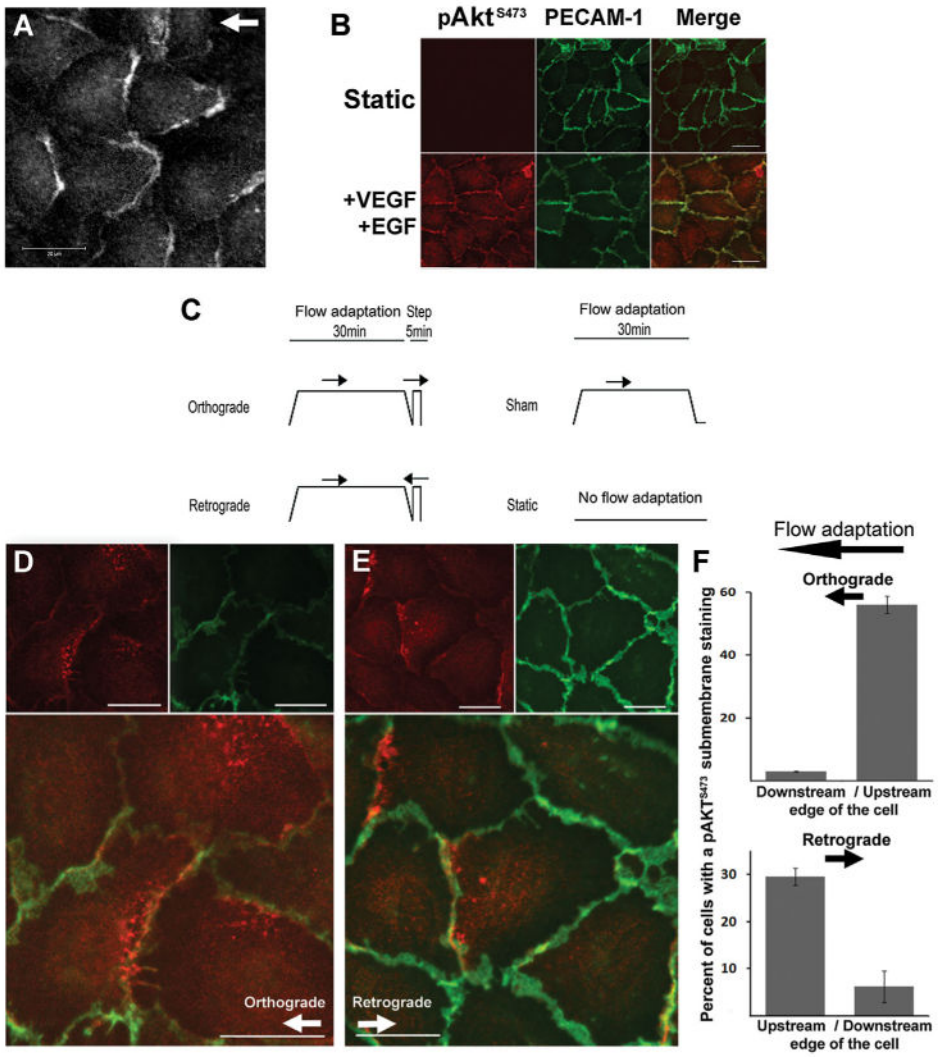

Fig. 2.

Cellular distribution of Akt-1 phosphorylation relative to the flow source. A: Serine 473 phospho-specific Akt-1 (pAkt-1^{S473}) immunostaining of HUVEC monolayers subjected to a 5 min step flow at 16 dyn cm^{-2}. B: pAkt-1^{S473} (red) costaining with PECAM-1 (green) in static control (upper panel) and after a 5 min stimulation 10 nM EGF plus 100 ng ml^{-1} VEGF (lower panels). C: Schematic of the protocols used for flow adaptation of monolayers consisting of a 30 min slow ramped flow up to 16 dyn cm^{-2} then ramped down, followed by a 5 min step flow in either direction. Sham monolayers were not subjected to a second step flow stimulation after flow adaptation but were left sealed on the flow chamber at 37°C for the last 5 min. Static slides were never removed from the incubator. D,E: costaining of pAkt-1^{S473} (red) and PECAM-1 (green) after 30 min flow-adaptation and 5 min ortho- (D) or retrograde flow (E). F: bar graph indicates fraction of cells with detectable submembrane pAkt-1^{S473} staining in both ortho- (upper) or retrograde (lower) flow conditions. Scale bars are 20μm; arrows indicate direction of flow.

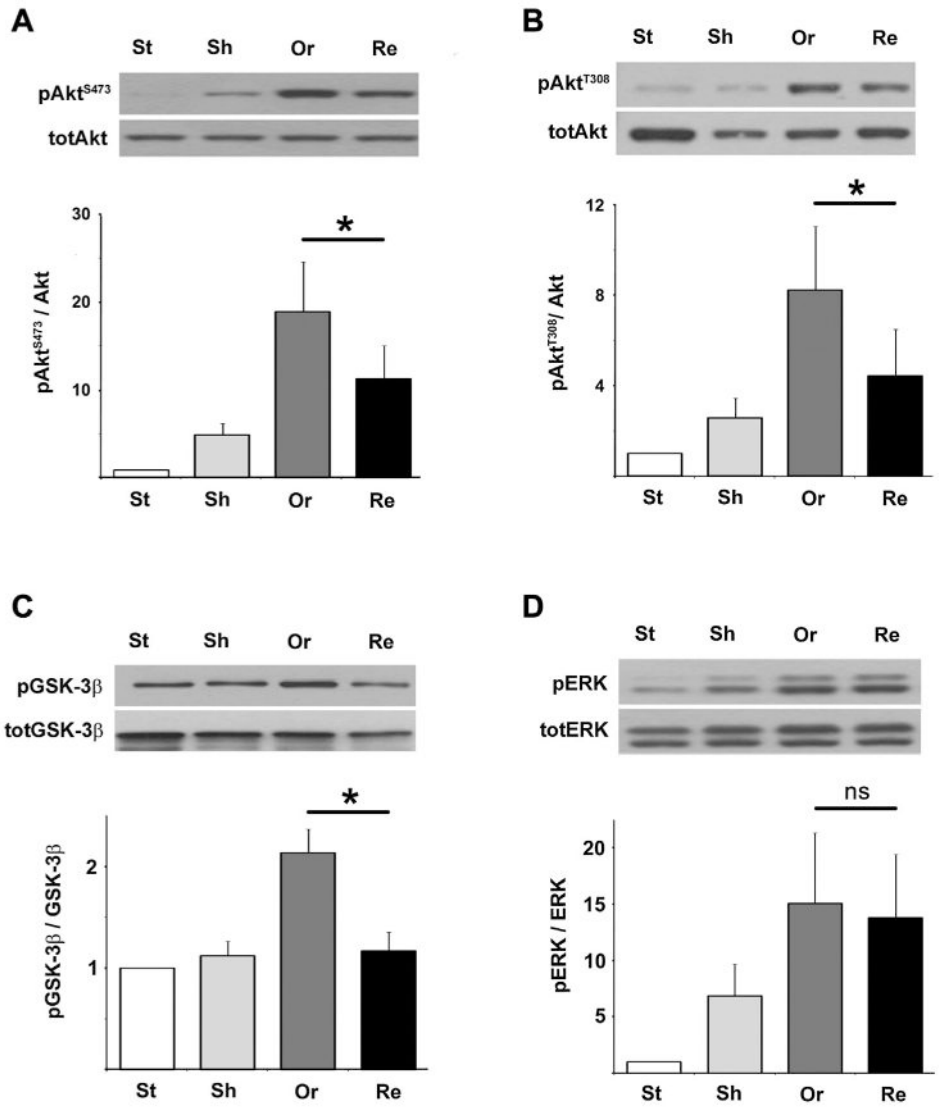

Fig. 3.

Akt-1 responses are attenuated when flow is reversed. A,B: Akt-1 phosphorylation at both S^{473} and T^{308} positions of flow-adapted HUVEC cells was significantly attenuated when a 5min reversal flow was applied (Retrograde: Re) compared to an orthograde flow (Or; *S^{473}: *P*= 0.002 and *T^{308}: *P* = 0.023, n = 9 and n = 7 individual experiments, respectively). C,D: Only an orthograde flow was able to induce phosphorylation of GSK-3β (C, **P*= 0.046, n = 4) while the Erk pathway responded to flow but was insensitive to the flow direction (Erk: *P*=0.19, n = 8; when comparing Or to Re, n = 4 individual experiments).

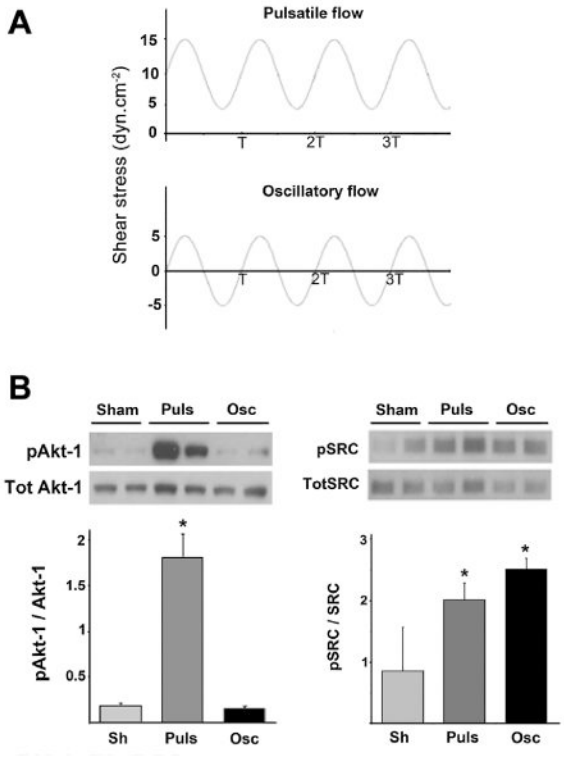

Fig. 4.

A forward flow component is required for flow-induced Akt-1 activation. A: Pulsatile (Puls) and oscillatory (Osc) flow were applied at similar frequency and amplitude of flow (10 dyn $cm^{-2,}$ T = 1 s). B: Akt-1 (S473) and Src (Y416) phosphorylation levels respectively in non-adapted HUVEC monolayers after 5 min of pulsatile or oscillatory flow or in sham-mounted slides (Sh). Ratio pAkt-1/Akt-1: Puls: 1.82 ±0.25, Osc: 0.15 ±0.01, P= 0.032. Representative blots with duplicates are shown above.

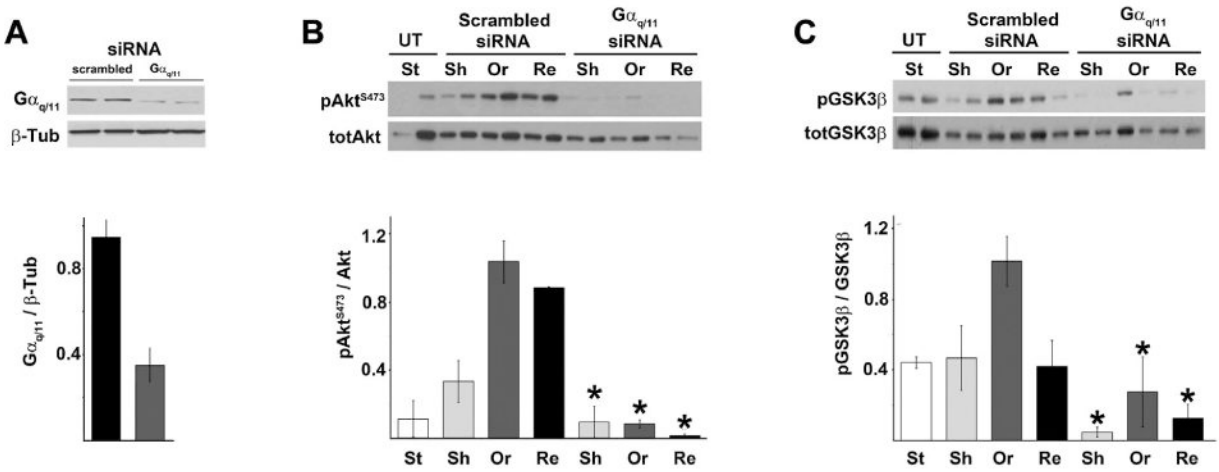

Fig. 5.

Silencing of $G\alpha_{q/11}$ was sufficient to abrogate flow-induced Akt-1 and GSK-3β responses. Cells were pretreated with siRNA against $G\alpha_{q/11}$ or with a scrambled siRNA then subjected to a 30 min of flow adaptation and a 5 min step ortho- (Or) or retrograde flow (Re) as described in Figure 2. A representative blot of an experiment performed with duplicates is shown above. A: $G\alpha_{q/11}$ siRNA silencing in primary HUVEC was measured by western blot as a ratio of total $G\alpha_{q/11}$ over β-tubulin (β-Tub). B,C: Effect of $G\alpha_{q/11}$ silencing on flow-induced Akt-1 phosphorylation at S^{473} and GSK-3β phosphorylation respectively (*P< 0.05 when compared to their scrambled siRNA treated counterpart). UT, untreated; St, static flow naïve; Sh, flow adapted sham.

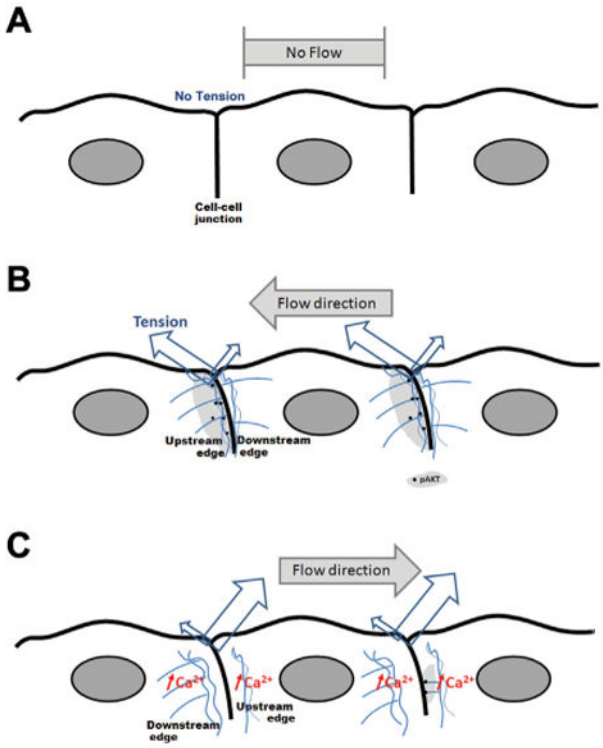

Fig. 6.

Relationship between subcellular pAkt-1 localization to shear stress, increased membrane tension, and actin cytoskeleton. As demonstrated by Fung and Liu [1993] and Melchior and Frangos [2010], the cell–cell junction adapts morphologically by inclination in direction of flow and the region immediately downstream of the junction is the site of greatest membrane tension. We propose that Akt-1 activation correlates with regions of high tension and an intact actin cytoskeleton. Thus, while no tension is present in static condition (A), an orthograde flow induces phosphorylation of Akt-1 at junctional upstream regions where tension is highest and the actin cytoskeleton is intact (light gray, B). C: Retrograde flow also produces high tension in the upstream region, but also induces increases in intracellular calcium [Melchior and Frangos, 2010] which destabilize/depolymerize the actin cytoskeleton (blue). Thus, retrograde flow leads to reduced upstream localization of pAkt-1.